Modelling of Distribution Level Coreless Induction Furnace for Rapid Voltage Change Assessment

T. Trummal, T.Sarnet, J.Kilter

***Abstract*—This paper proposes a mathematical model for a distribution level, directly fed core-less, induction furnace that can be used for network voltage behavior related studies performed by the network operators. The objective of the model is to represent the dynamic behaviour of the facility when an induction furnace is energized (switched) at the beginning of the melting process. Model development is supported by actual field measurements from PCC to a distribution system. The paper includes a case study and the results indicate that the proposed model offers accurate results for rapid voltage change assessment and it is shown that the model can be successfully used for various load changes and at various voltage levels.**

***Keywords*—connection study, core-less induction furnace, distribution network, rapid voltage change**

I. Introduction

INDUCTION furnaces are electrical furnaces where the heat is applied using electromagnetic induction. These furnaces are used by the foundries and metallurgy plants for melting different metals, e.g. iron, steel, aluminum. Due to inherent characteristics of these type of loads they are often considered as one of the most challenging electrical installations from the viewpoint of power quality. These challenges are related harmonic distortion, voltage flicker and fluctuation including rapid voltage changes (RVCs), and voltage unbalance (depending on connection type). Harmonic distortion can cause excess heating and damage to equipment connected to the network, e.g. cables, transformers, motors. RVCs, flicker and fluctuations can disrupt the operation of voltage sensitive clients of the power system. Considering this it is essential to thoroughly assess these type of loads when connected to electrical network.

For the purpose of power quality related studies and assessment the induction furnace type of loads are usually modelled as a resonant RLC circuit. The values for the circuit are usually derived from field measurements. In order to describe steady-state fluctuations during melting process a time-varying component can be added. This resonant circuit is then interfaced with rest of the power system according to the type of furnace. This modelling approach has been used in [1]–[5].

All of these referenced papers assess the steady-state behaviour of induction furnaces, but on the other hand the dynamic behavior analysis of these loads have not been so prevalent. However, for actual systems and new connection application assessment dynamic behaviour of these loads is also of relevance as the operation of a furnace can cause RVCs. In Europe, the limits for supply voltage characteristics, including harmonics, RVCs, unbalance, etc. are given in standard EN 50160 [6]. For example, understanding the influence of RVCs is important as these can cause control system malfunction or incorrect operation of electronic equipment [7], e.g. distributed generation controllers.

There are different types of induction furnaces meant to process different materials at different volumes. This paper concentrates on core-less induction furnace at distribution level and on its modelling and analysis aspects with respect to connection to the grid and cooperation with other nearby plants. The objective here is to derive an approach and respective model that can be used to perform connection studies and obtain preliminary understanding of how this type of load influences the network and other customers connected to same or nearby substations. Based on this understanding it is possible to derive limitations or alternatives connection measures to guarantee appropriate network operation and fulfillment of respective power quality limits.

This paper is divided into three sections. In Section II overview of coreless induction furnace, its' influence on power system and modelling approaches are explained. Section III describes the proposed model including the methodology that is used to derive model equations from field measurements. Performance of the proposed model is assessed in Section IV. The paper ends with conclusions.

II. Background

A. Induction Furnace Types

The principle of induction melting [8] is about transferring the heat in the form of electrical current to melt different metals and alloys. This is made using the high voltage source of a primary coil that induces a low voltage, high current in the metal or secondary coil. Induction furnaces have different types of constructions and power supplies depending of their purpose, the metal or alloy they are used to process and the volume of processed metal. Induction furnaces can be classified by their construction as [8], [9]: i) core type, ii) core-less type, and iii) channel type. This paper is focused on core-less induction furnaces. Core and channel type furnaces are explained in references [8], [10].

Core-less type induction furnace consists of heat-resisting crucible encircled by a solenoid coil that is fed from single phase power supply. The fluctuating axial magnetic field linking the charge within the crucible causes Joules heating within it. Additionally the coil can be hollow to allow water cooling to reduce the losses during melting process. There are two options for power supply for these furnaces: i) direct supply from the network (mains frequency supply type) to the

Paper submitted to the International Conference on Power Systems Transients (IPST2021) in Belo Horizonte, Brazil June 6-10, 2021.

furnace through a furnace transformer or ii) power electronics (PE) based connection to rise the operating frequency of the furnace or use DC voltage as supply. PE-interfaced furnaces usually use three-phase AC to DC and DC to one-phase AC conversion. Core-less type induction furnaces can be classified by the type of their power supply as following [9], [11]: i) mains frequency (50/60 Hz), ii) low frequency (up to 500 Hz), iii) medium frequency (500...1000 Hz), iv) high frequency (2500 Hz and higher), and v) direct current.

Furnaces operating at mains frequency offer efficiencies between 60% and 85%. Higher frequency power supply is used to enhance the efficiency (up to 95%) of the furnaces and therefore allow more energy intensive melting processes. However, lower frequency furnaces offer better conditions for mixing of alloys and better quality end products. This means that as a rule of thumb [9], the operating frequency of the induction furnace decreases inversely to the capacity of the furnace. There is also research on dual-frequency core-less type induction furnaces [12] where the furnace is fed by both lower and higher frequency power supplies. Here the higher frequency is used to melt the solid metals and lower frequency to finish the process to achieve better quality end products.

B. Influence of Induction Furnaces on Power System Operation

Induction furnaces cause power quality disturbances during their operation. The most significant of them are harmonics and RVCs. During melting process the changing resonant frequency of the coil injects harmonic distortion to the grid. This issue is further magnified due to the time-varying nature of current harmonic orders and magnitudes injected to the grid. [5] This can mean that the harmonic distortion can be significant and according to the measurements presented in [1] the voltage THD can even be higher than 70%.

Induction furnace is in essence a varying load as the operating cycles are alternating. This inherently causes voltage flicker and fluctuations [5]. Furthermore, the furnace is energized when the melting process start and this can lead to the emergence of RVCs. RVC is classified as a power quality event [13] that is defined as and characterized by small and fast transition between two steady-state voltage levels. RVCs usually result from different switching operations, e.g. motor starting, fast load or generation changes, or transformer tap changes. In the distribution network RVCs are becoming more prevalent due to the increasing penetration of dynamic loads and renewable generation. For example, in Europe the fluctuating loads are governed by European standard EN 50160 [6] and IEC standard 61000-3-7 [13]. However in other countries other relevant standards may apply. Furthermore network operators can set their own target for emission levels. In this paper RVC is calculated as [6], [13]:

$$\Delta V_{\%} = \frac{V_{before} - V_{min}}{V_{before}} \cdot 100\%, \tag{1}$$

where V_{before} is the voltage value before and V_{min} is the voltage minimum during switching process of an induction furnace.

C. Modelling of Induction Furnaces

In the literature the furnaces (mostly PE-interfaced) are usually modelled using parallel resonant RLC circuit, where C represents the resonance capacitor bank, and R and L the furnace coil. This model is then connected to the network using power electronics i.e. rectifiers. This method is used for example in [1]–[5]. Field measurements from terminals of an induction furnace are usually used to derive the R, L and C values. A time-varying component [5] that describes the steady-state fluctuations of a furnace during melting process can be added to the R and L values. However, these models do not take into account the dynamic behaviour of the furnace when it is energized at the start of the melting process.

The easiest way to implement this dynamic behaviour is to use measured values from an induction furnace. The measurements are then imported to an EMT environment where they are played back. Depending on the purpose of the study active and reactive power, current rms or current wave-forms can be used. Another approach is to approximate the load changes using a suitable function.

A variation of the model in [5] is proposed in this paper. The same time-varying resistance and inductance method is implemented to represent the energising of the induction furnace. In this paper another modification is used and the measurements from a PCC are used instead of the ones from furnace terminals. This approach is more suitable for the network operators as measurements from the PCC can be obtained in more easier way. Also it is possible to use existing measurement devices that are capable to perform wave-form measurements, e.g. fault recorders.

D. Field Measurements of an Induction Furnace Facility

An induction furnace facility at distribution level is observed in this paper (Fig. 1). This facility uses three core-less mains frequency induction furnaces with nominal capacities of 0.4, 1.0 and 1.6 MVA. The furnaces are combined units where furnace transformers and induction furnaces are integrated into single unit that can be connected to the power system with transformer terminals. The facility is connected to the PCC by a short cable line.

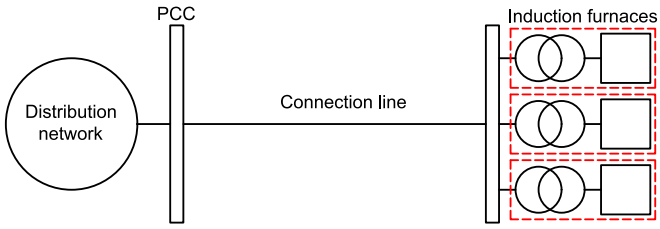

Fig. 1. Connection of the induction furnace facility to the distribution network. Induction furnaces are circled with red dashed line.

The measurement campaign was carried out at the PCC. This means that full facility load including furnaces and furnace transformers are aggregated at the PCC. Current and voltage wave-forms were sampled at 20 kHz. Example of load and voltage changes due to switching of an induction furnace

are presented on Fig. 2. It can be seen that switching of an induction furnace causes sudden load and voltage changes. In the example the load is increasing by around 0.5 MVA which causes a peak of around 3.7 MVA in apparent power. Calculated RVC is 5.1%.

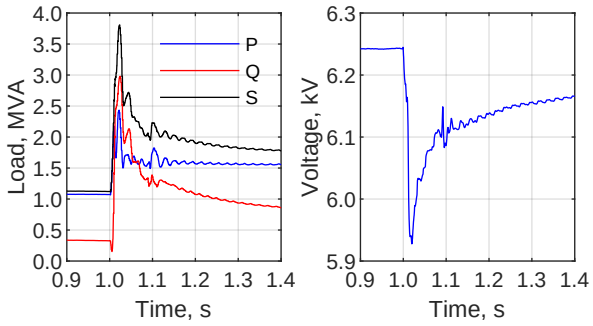

Fig. 2. Example of load and voltage changes due to operation of induction furnace in the facility.

III. Induction Furnace Dynamic Model Development

The aim of the proposed mathematical model of induction furnace is to describe load changes when a core-less mains frequency induction furnace at distribution level is switched on (hereafter called as RL model). This model is designed as a parallel RL load model. Measurements given on Fig. 2 are used and three-phase equivalent resistance and inductance of the induction furnace facility are calculated (Fig. 3). The time-series can be divided into two parts: i) steady-state and ii) dynamic-state. The steady-state part is described in Section III-A. Derivation of the dynamic-state part is given in Section III-B. Scaling and final form of the RL model are given in Section III-C and Section III-D, respectively.

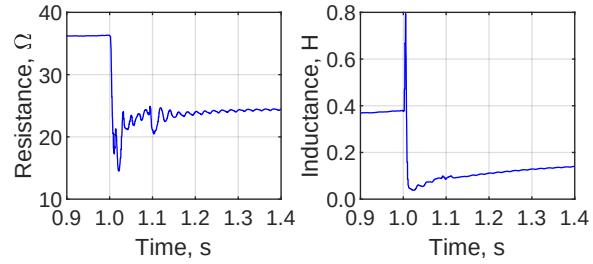

Fig. 3. Calculated equivalent resistance and inductance of the induction furnace facility.

A. Steady-State Part of the Proposed Model

In RL model the steady-state operation of an inductance furnace is described using a constant resistance and inductance that are noted as R_{steady} and L_{steady}. This is the starting load of the induction furnace facility at the beginning of the simulation. Suitable starting constants can be easily calculated using equations (2) and (3).

$$R_{steady} = \frac{\sqrt{3} \cdot V^2}{P}, \tag{2}$$

$$L_{steady} = \frac{\sqrt{3} \cdot V^2}{Q \cdot 2\pi f_n}, \tag{3}$$

where V is operating voltage, P active power and Q reactive power of the induction furnace and f_n is nominal frequency of the power system. Here P and Q are the load of the facility before a furnace is switched on, and range from 0 to nominal capacity minus one furnace.

B. Derivation of Equations for Dynamic-state Part of the Proposed Model

The equations describing the dynamic operation of the induction furnace are derived using regression analyses. Consider a data set obtained from measurements consisting of the m data points

$$(x_1, y_1), (x_2, y_2), \ldots, (x_m, y_m). \tag{4}$$

The main objective of the non-linear least squares method [14], [15] is to find a curve y described by the function

$$y = f(x, \beta), \tag{5}$$

which optimally represents the data set. The curve is a function of the independent variable x and the vector β of n parameters

$$\beta = (\beta_1, \beta_2, \ldots, \beta_n) \tag{6}$$

so that the condition $m \geq n$ is respected.

The curve is fitted to the data by finding appropriate values of β that minimize the sum of squares S calculated as

$$S = \sum_{i=1}^{m} r_i^2, \tag{7}$$

where r_i are the residuals and can be obtained using

$$r_i = y_i - f(x_i, \beta). \tag{8}$$

The residuals are the differences between the values of the dependent variable (y_i) and the correspondent values of the model ($f(x_i, \beta)$).

The sum of squares is minimized iteratively by calculating the set of n gradient equations

$$\frac{\partial S}{\partial \beta_j} = 2 \sum_i r_i \frac{\partial r_i}{\partial \beta_j} = 0 \qquad j = 1, \ldots, n. \tag{9}$$

The number of gradient equations is n as the model contains n parameters. The sum of squares reaches its minimum value when the gradient is zero.

The reason an iterative solution is selected is due to the nonlinearity of the model where the derivatives $\frac{\partial r_i}{\partial \beta_j}$ contain both the independent variables and parameters. Before the first iteration, a set of initial values must be chosen for the parameters. These values are then refined as a result of the iterations. This is expressed by the following equation

$$\beta_j = \beta_j^k + \Delta\beta_j, \tag{10}$$

where k is number of iteration and $\Delta\beta_j$ the increment of the iteration. The model is linearized at each iteration by approximation to a first-order Taylor polynomial expansion.

$$\begin{aligned} f(x_i, \beta) \approx f(x_i, \beta^k) + \sum_j \frac{\partial f(x_i, \beta^k)}{\partial \beta_j} (\beta_j - \beta_j^k) = \\ = f(x_i, \beta^k) + \sum_j J_{ij} \Delta\beta_j. \end{aligned} \tag{11}$$

where the Jacobian J_{ij} is a function of constants (the independent variable and the parameters) and is given by

$$J_{ij} = -\frac{\partial r_i}{\partial \beta_j}. \tag{12}$$

The residuals in this case are calculated as

$$\Delta y_i = y_i - f(x_i, \boldsymbol{\beta}^k) \tag{13}$$

and

$$r_i = y_i - f(x_i, \boldsymbol{\beta}) \approx \Delta y_i - \sum_{s=1}^{n} J_{is} \Delta \beta_s. \tag{14}$$

This is then substituted into (9), resulting in

$$-2 \sum_{i=1}^{m} J_{ij} \left(\Delta y_i - \sum_{s=1}^{n} J_{is}\ \Delta \beta_s \right) = 0. \tag{15}$$

If this expression is rearranged, n simultaneous linear equations are obtained. These equations are also called normal equations and are given by

$$\sum_{i=1}^{m} \sum_{s=1}^{n} J_{ij} J_{is}\ \Delta \beta_s = \sum_{i=1}^{m} J_{ij}\ \Delta y_i \qquad j = 1, \ldots, n. \tag{16}$$

The normal equations can be written in matrix notation as

$$\left(\mathbf{J^T J}\right) \boldsymbol{\Delta \beta} = \mathbf{J^T}\ \boldsymbol{\Delta y}. \tag{17}$$

The iterative method described is repeated until the required convergence precision ε is reached. This is calculated after every iteration and expressed by

$$\left| \frac{\Delta \beta_j}{\beta_j} \right| < \varepsilon, \tag{18}$$

For instance, if the convergence precision is chosen as 0.0001, each parameter should be refined to 0.1% precision.

Non-linear least squares regression analyses can be implemented with multiple commercially available softwares. In this paper, the built-in curve fitting tool provided in MATLAB is used. Different functions were considered in order to fit the resistance and inductance data to a curve. In this paper rational function is chosen for curve fitting.

A rational function is a ratio of two polynomials and it can be represented as

$$y = \frac{p_n x^n + p_{n-1} x^{n-1} + \ldots + p_2 x^2 + p_1 x + p_0}{q_m x^m + q_{m-1} x^{m-1} + \ldots + q_2 x^2 + q_1 x + q_0}, \tag{19}$$

where p and q are the rational coefficients, n denotes a positive integer that defines the degree of the numerator and m denotes a non-negative integer that defines the degree of the denominator.

Non-linear least squares curve fitting method described previously is applied to resistance and inductance time-series. This means that for resistance (4) and (5) can be written as

$$(t_1, r_1), (t_2, r_2), \ldots, (t_m, r_m) \tag{20}$$

and

$$R = f(t, \beta_r). \tag{21}$$

Same thing can be written for inductance as

$$(t_1, l_1), (t_2, l_2), \ldots, (t_m, l_m) \tag{22}$$

and

$$L = f(t, \beta_l). \tag{23}$$

where β_r and β_l are vectors representing the coefficients of the rational functions fitting the resistance and inductance data points, respectively. After experimenting with different degrees of rational functions the best fit can be achieved with linear/quadratic rational function for resistance and linear/quadratic for inductance. Coefficient of determination (also known as R^2 or R-squared) is used to assess how well the curve fits the data points.

The curve fitting method was applied and the functions representing the resistance and inductance were obtained as

$$R(t) = \frac{96280 \cdot t + 305}{t^4 - 11.65 \cdot t^3 + 37 \cdot t^2 + 3954 \cdot t - 24}, \tag{24}$$

$$L(t) = \frac{2 \cdot t + 0.24}{t^2 + 7.32 \cdot t + 4.19}, \tag{25}$$

where t is time in seconds and where $t = 0$ s represents the time of switching on an induction furnace. Suitable time for switching can be set by using an offset (switching at $t = 1$ s is achieved by offset of -1). The resulting R-squared values for the functions (24) and (25) are 0.966 and 0.853, respectively.

These equations (24) and (25) obtained from the curve fitting describe how the induction furnace facility behaves when an induction furnace is switched on. Due to the switching, the RL model presents a time-dependant behavior. In other words, the equations show that the resistance and inductance do not remain constant over time.

C. Voltage and Load Scaling of the Proposed Model

The derived equations only apply for specific voltage level and load change. A scaling factor must be added to the equations to derive voltage and load dependent RL model. Voltage scaling can easily be implemented by ratio of required voltage squared to measured voltage squared. However, with active and reactive power it is a bit more complicated as the resistance R and inductance L are inversely proportional to active power P and reactive power Q, respectively. Another aspect to consider is that the load scaling factor should factor in the load change not the load value after the switching. This means that the scaling factor for the load change must be approximated with some equation. The easiest way to do is to scale the original equations with a scaling factor and record the active and reactive power change for each scaling. This data is then plotted and analyzed. Afterwards, the data is then linearized with a linear function. Final scaling factors for the RL model are given below:

$$F_R(V, P) = \frac{V^2}{V_m^2} \cdot \frac{1}{0.888 \cdot P_s + 0.567}, \tag{26}$$

$$F_L(V, Q) = \frac{V^2}{V_m^2} \cdot \frac{1}{1.369 \cdot Q_s + 0.521}. \tag{27}$$

where V_m is the measured voltage, V is the operating voltage of the induction furnace, P_s and Q_s are the differences between two steady-state values i.e. before and after switching.

D. Final Form of the Proposed Furnace Model

Final equations that describe the dynamic-state operation of a core-less mains frequency induction furnace when it is switched are given as following:

$$R(t,V,P) = \frac{V^2}{34.7 \cdot P_s + 22.1} \cdot \frac{96280 \cdot t + 305}{t^4 - 11.65 \cdot t^3 + 37 \cdot t^2 + 3954 \cdot t - 24}, \quad (28)$$

$$L(t,V,Q) = \frac{V^2}{53.5 \cdot Q_s + 20.4} \cdot \frac{2 \cdot t + 0.24}{t^2 + 7.32 \cdot t + 4.19}. \quad (29)$$

These two equations together with equations (2) and (3) form the RL model of a core-less mains frequency induction furnace. As there are two parts (steady and dynamic state) there must be a switch implemented to switch from steady state to dynamic state at the time when switching of an induction furnace is desired.

IV. Case Study and Results

The performance and accuracy of the proposed RL model described in Section III is studied using a case study based on a Estonian urban distribution network. The RL model and the case study network is implemented in EMT environment.

A. Description of the Studied Distribution Network

The case study network with the induction furnace facility (briefly described in Section II-D) is shown on Fig. 4. The network has 2 nominal voltages: 110 kV and 6 kV, and is fed from the transmission network through line L1 at 110 kV. The 6 kV network has two substations S_1 and S_2 that are connected by short cable lines L2 and L3. Both substations have their load aggregated to the busses of the respectable substation, other than the induction furnace facility of course. The induction furnace facility is connected at 6 kV with PCC at substation S_2. The facility also owns a cable line L4 that connects the facility itself with the PCC.

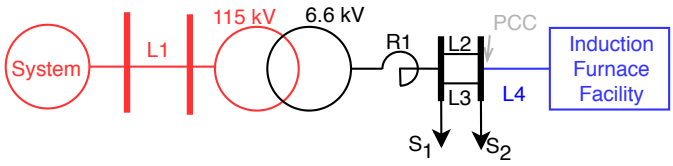

Fig. 4. Single line diagram of the studied power system (red – 110 kV transmission system, black – 6 kV distribution system, blue – induction furnace installation).

Three cases are studied to analyze the performance of the RL model. Case 1 implements the RL model on the case study network. Modelling method where measured current wave-forms are fed into the simulation using current sources (hereafter called as wave-from model) is also implemented in Case 1. The results of these two models are compared. Case 2 implements the load scaling of the RL model on the case study network, where the load change is scaled between 0.4...5 MVA. Case 3 implements the voltage scaling of the RL model and analyzes the scalability of the RL model at different voltage levels. This is implemented by connecting the RL model with a three-phase source.

B. Case 1 and Results

Results of Case 1 are presented on Fig. 5. Here, the results of the RL model are compared to the results of the wave-form model. The average voltage error is 0.07 % (for $t = 0.5 \ldots 7$) and maximum 1.16 % when compared to the wave-form model. It can be seen that the voltage of RL model closely follows the voltage of the wave-form model. Therefore it can be said that the RL model is suitable for assessing RVCs. In this case the RVC is 3.54 % for the RL model 4.25 % for the wave-form model. The results show that the RL model is somewhat conservative. Regardless of this it can be argued that the dynamic behaviour is adequately represented with equations (28) and (29).

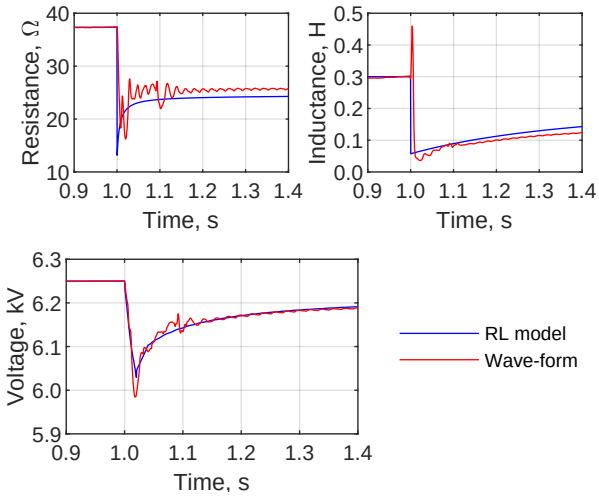

Fig. 5. Results of the simulation: top – voltage at PCC, center – resistance of the induction furnace, bottom – inductance of the induction furnace. Results of the RL model are in blue and wave-form model in red.

C. Case 2 and Results

Results of Case 2 are presented in Table I. In this case the load is scaled from 0.4 to 5.0 MVA and the difference between the desired load change (S_{reg}) and simulated load change (S_{sim}) are analyzed. It can be seen that the RL model has quite a good scalability between 0.7...5 MVA, as the average error is around 5%. However at lower capacities the scaling accuracy declines. This could be explained by the fact that the scaling factor for the load is approximated as a linear function.

TABLE I
Case 2 Results: Load Scalability of the RL Model

S_{reg}, MVA	S_{sim}, MVA	Error, MVA	Error, %
0.4	0.328	-0.072	-18.1
0.7	0.666	-0.034	-4.9
1.0	1.000	0.000	0.0
1.6	1.686	0.086	5.4
2.0	2.132	0.132	6.6
3.0	3.202	0.202	6.7
4.0	4.216	0.216	5.4
5.0	4.175	0.175	3.5

D. Case 3 and Results

Results of Case 3 are presented in Table II. In this case the operating voltage of the induction furnace is scaled for different voltage levels that are used in Estonian distribution networks. In this case the RL model is connected to a three-phase voltage source as described before. A load change of 1 MVA is applied and the difference of the desired and simulated load change (S_{sim}) is analyzed. It can be seen that the scaling of the voltage is as good as with load scaling with average error of around 4%.

TABLE II
CASE 3 RESULTS: VOLTAGE SCALABILITY OF THE RL MODEL

U_N, kV	S_{sim}, MVA	Error, %
6	0.969	-3.1
10	1.024	2.4
20	1.044	4.4
35	1.050	5.0
110	1.053	5.3

E. Discussion

The results show that the RL model has an average voltage error of 0.07% and maximum error of 1.16% when compared to the wave-form model. Scaling of the model for different capacities and voltages can offer satisfactory results but the average error is around 4...5%. This error could have multiple possible sources. First being that the scaling factor for load change is approximated by a linear function. Second being that the voltage scaling is very sensitive to the difference between the desired voltage and operating voltage.

Additional calculations have been made to study the impact of the cable line between the furnace facility and PCC. Respective results are presented in Fig. 6. It is shown that various cable lengths (0 km, 1 km and 2 km) have limited effect on the results. MAPE compared to 0 km cable length result is 0.0225% for 1 km and 0.0447% for 2 km. Moreover, the difference in RVC-s can also be considered as limited (here 0 km is taken as the actual value): 0.61% for 0.5 km, 1.25% for 1 km and 2.58% for and 2 km.

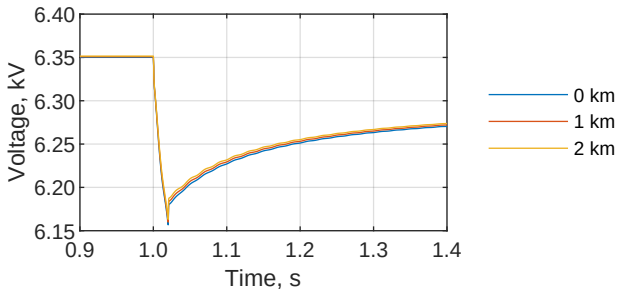

Fig. 6. Voltage at PCC for different cable lengths (0 km, 1 km and 2 km).

V. CONCLUSIONS

This paper proposes a model for a directly fed mains frequency core-less induction furnace at distribution level. The model is divided into two parts: steady and dynamic state and is designed as a parallel resistance and inductance circuit. Steady-state part of the model describes the starting load of the model. Dynamic part is implemented by a time-varying component.

The proposed RL model is studied using case study based on an Estonian urban distribution network. The cases show that the RL model offers satisfactory results and can be considered as a suitable tool for induction furnace induced RVC assessment.

VI. REFERENCES

[1] T. S. Saggu, L. Singh, and B. Gill, "Power quality improvement in induction furnace using eleven level cascaded inverter based DSTATCOM," in *2016 IEEE Electrical Power and Energy Conference (EPEC)*, IEEE, Oct. 2016.

[2] G. A. Patil, Y. N. Bhosale, and V. S. Bolaj, "Passive filter design to mitigate harmonics in three phase induction furnace," in *2017 International Conference on Circuit ,Power and Computing Technologies (ICCPCT)*, IEEE, Apr. 2017.

[3] T. S. Saggu, L. Singh, and B. Gill, "Application of UPQC for power quality improvement in induction furnace," in *2018 IEEE/IAS 54th Industrial and Commercial Power Systems Technical Conference (I&CPS)*, IEEE, May 2018.

[4] G. Stefanov, L. Karadzinov, and D. Karanfilov, "Design of power converter for induction furnaces with computer simulations," in *The 33rd International Convention MIPRO*, 2010.

[5] İ. Yilmaz, M. Ermis, and I. Cadirci, "Medium-frequency induction melting furnace as a load on the power system," *IEEE Transactions on Industry Applications*, vol. 48, no. 4, pp. 1203–1214, 2012.

[6] "Voltage characteristics of electricity supplied by public electricity networks," CENELEC, Standard EN 50160, 2010.

[7] J. Schlabbach, D. Blume, and T. Stephanblome, *Voltage Quality in Electrical Power Systems*. Institution of Engineering and Technology, Nov. 1, 2001, 252 pp., ISBN: 0852969759.

[8] M. A. Laughton, *Electrical engineer's reference book*. Oxford England Boston: Newnes, 2003, ISBN: 9780080523545.

[9] Студопедия, *Плавка чугуна в индукционных печах*, [Online]. Available at https://studopedia.su/9_66919_plavka-chuguna-v-indukts ionnih-pechah.html. Accessed: 28.10.2020. [in Russian].

[10] Small Business Magazine, *Understanding the types of core and coreless induction furnace*, [Online]. Available at https://smallbusin essmagazine.org/understanding-the-types-of-core-and-coreless-induct ion-furnace/. Accessed: 28.10.2020.

[11] J. Choi, S. K. Kim, S. Kim, K. Sim, M. Park, and I. K. Yu, "Characteristic analysis of a sample HTS magnet for design of a 300 kW HTS DC induction furnace," *IEEE Transactions on Applied Superconductivity*, vol. 26, no. 3, pp. 1–5, 2016.

[12] V. E. Frizen, V. I. Luzgin, A. S. Koptyakov, K. E. Bolotin, N. V. Tarchutkin, and S. E. Mironov, "Induction crucible furnace with dual frequency power supply," in *2017 15th International Conference on Electrical Machines, Drives and Power Systems (ELMA)*, 2017, pp. 423–426.

[13] "Electromagnetic compatibility (EMC) – part 3-7: Limits – assessment of emission limits for the connection of fluctuating installations to MV, HV and EHV power system," IEC, Standard IEC 61000-3-7:2008, 2008.

[14] C. Rao, *Linear models: least squares and alternatives*. New York: Springer, 1999, ISBN: 0387988483.

[15] A. Abba, A. Manenti, A. Suardi, A. Geraci, and G. Ripamonti, "Non-linear least squares fitting in FPGA devices for digital spectroscopy," in *2009 IEEE Nuclear Science Symposium Conference Record (NSS/MIC)*, 2009, pp. 563–568. DOI: 10.1109/NSSMIC.2009 .5401957.